14th IEA Heat Pump Conference
15-18 May 2023, Chicago, Illinois

Investigation of industrial high-temperature heat pumps for simultaneous heating and cooling: A brewery case study

Martin Pihl Andersen[a], Roger Padullés I Solé[a], Benjamin Zühlsdorf[b], Wiebke Brix Markussen[b], Jonas Kjær Jensen[a], Brian Elmegaard[a]

[a]Department of Civil and Mechanical Engineering, Technical University of Denmark, Kgs. Lyngby, 2800, Denmark
[b]Danish Technological Institute, Taastrup, 2630, Denmark
*Corresponding author, mapian@dtu.dk

Abstract

Process industries are responsible for a large share of the global energy demand. While refrigeration systems are used in the industry for the supply of cooling, the introduction of high-temperature heat pumps (HTHPs) and electric boilers to supply heat is necessary for the electrification of this industry. Combining the refrigeration system and the HTHP may offer an opportunity to improve the overall efficiency and facilitate the integration of HTHP. However, fluctuating, and non-continuous demands make the integration of a combined heat pump for simultaneous heating and cooling (HPS) more challenging as the heating and cooling capacity for such a system is coupled.
This study compared a cascade HPS with an R-717 bottom cycle and R-718 top cycle to a reference system consisting of a R-717 refrigeration system releasing excess heat to the ambient and a HTHP with R-717 and R-718 using the ambient as a heat source. The HPS configuration included heat exchangers with ambient air, and ambient heat sources to meet all combinations of heating and cooling demands. The comparison was carried out for an industrial brewery case and was based on numerical modelling.
For each combination of heating and cooling load the usage of ambient air as heat source and sink was adapted and simultaneously the pressure levels in the HPS were optimized for minimum electricity consumption. The influence of the ambient temperature was also analysed.
At design conditions the electricity consumption of the HPS was 9.8 % lower than the electricity consumption of reference system, but only 2.1 % lower on a yearly basis, due to the fluctuating demand profiles. This indicates that the HPS did not offer a substantial improvement in in terms of thermal efficiency compared to the reference system.

Selection and/or peer-review under the responsibility of the organizers of the 14th IEA Heat Pump Conference 2023.

Keywords: industry; high temperature; heat pump; cooling; HPS

1. Introduction

Process industries are responsible for a large share of the global energy demand and comparably large CO_2 emissions. According to [1], 69 % of the European industry's energy consumption is used for process heating and cooling, with 40 % being delivered at temperatures below 200 °C. These processes show great potential for electrification, and through this reducing overall greenhouse gas emissions [2].

Refrigeration systems based on vapour compression cycles have been used in the industry for the supply of cooling since the mid-19th century [3] but the introduction of high-temperature heat pumps (HTHPs) and electric boilers to supply heat is not as prevalent in today's market in comparison. Nevertheless, HTHPs are an efficient and feasible solution for the total electrification of this industry [4]. However, increasing the temperature lift of the HTHPs to reach higher supply temperatures yields a lower coefficient of performance (COP) resulting in higher operating expenses (OPEX) challenging the economic potential.

Combining the refrigeration system and the HTHP into a single heat pump for simultaneous heating and cooling (HPS) offers an opportunity to improve the overall efficiency of delivering heating and cooling requiring one system instead of two [5]. However, the part-load performance of such systems has not been

analysed. At the same time, the existing cooling utility could be fully or partly replaced facilitating the electrification of the industry.

When operating a HPS, two thermal energy streams, one for cooling and one for heating, are produced simultaneously. Therefore, it is interesting for the user that the HPS operates in simultaneous mode as much as possible. However, the energy demand of industrial processes varies throughout the day.

The combination of batch processes and continuous demands dictates load variations on an hourly and daily basis [6], but weekly and seasonal variations also exist. As the heating and cooling capacity of the HPS are coupled, either heating or cooling will be in excess in most operating conditions when fulfilling the needed heating and cooling demands of the processes. The HPS will therefore either expel the excess to the ambient or fill a thermal storage. However, for large demand variations like seasonal trends, a thermal storage requires substantial amounts of space [7]. The HPS needs to adapt its operation to fulfil its function. Hence, the variability of the non-continuous energy demands makes the integration of a HPS more challenging where both operation during design conditions and during part-load are essential.

This study conducted a case study of supplying simultaneous heating and cooling with a HPS for a Danish brewery. The analysis was based on daily average consumption data assuming that daily variations were covered by existing heat storages. The HPS was designed to cover all demands of cold- and hot water with no further required utilities. The daily and yearly operations were evaluated in terms of electricity consumption and Lorenz efficiency, while being compared to a reference system which consisted of two separate utilities, a HTHP and a refrigeration cycle, respectively.

2. Method

This section presents the method and concepts used for the modelling, analysis, and evaluation of the HPS. First, the investigated case study is presented followed by the thermodynamic modelling of the HPS system and the reference system. Finally, relevant performance indicators are introduced which were used to assess this strategy for electrifying industrial processes.

2.1. Brewery case study

The industrial facilities chosen for this study was a Danish brewery producing a large variety of products. The consumption data and the ambient temperature for the year 2021 was used in the case study. The heating demand of the actual production facilities was traditionally covered by a natural gas boiler supplying hot water. The cold water was supplied by a refrigeration plant covering the cooling of products both during production and storage. The demand profiles used are presented in Figure 1 together with the ambient temperature. The orange curve shows the heat load, the blue curve shows the cooling load, and the grey curve shows the ambient temperature.

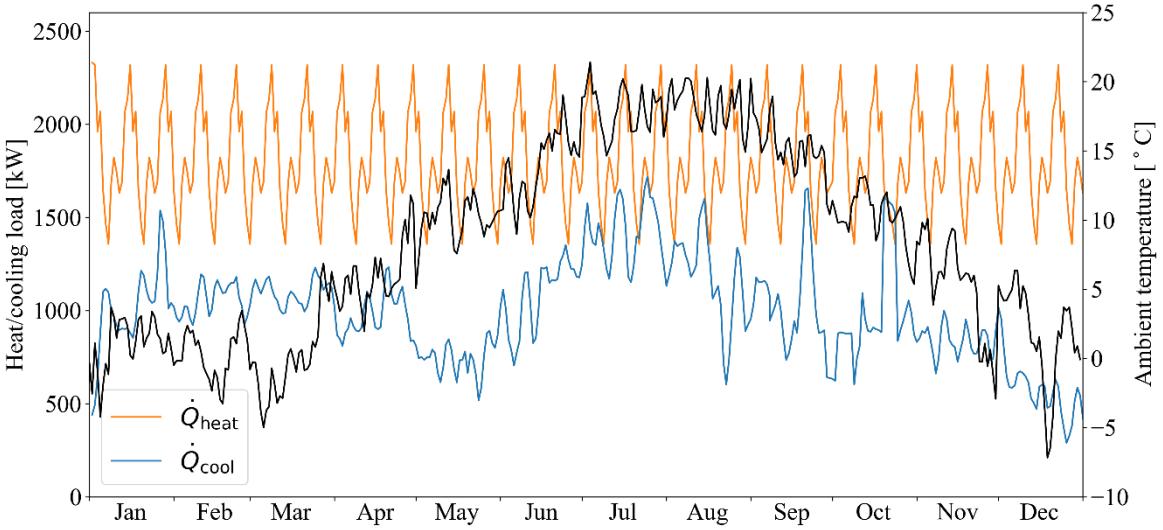

Figure 1: Daily average heating and cooling load supplied by hot water and cold water, respectively. The daily average temperature is presented on the secondary axis.

The heating demand follows a bi-weekly schedule with very little influence from the season. The demand fluctuates between 1350 kW and 2330 kW depending on the day. The demand for cold water follows a seasonal trend with lower loads during colder months. The cooling load is also low in May due to the product being transported directly to the customers to a higher degree. The demand varies between 290 kW and 1720 kW. This means that the ratio between the heating and the cooling demand is largest during the winter and smallest during the summer. The ambient changes with a seasonal trend between -7 °C and 21 °C.

The hot water is produced at a temperature of 145 °C by reheating the return water at 110 °C. The cold-water supply temperature is 2 °C while it returns at a temperature of 8 °C as presented in Table 1. The design cooling load of the HPS was chosen as 80 % of the maximum cooling demand, i.e., 1380 kW. The design heat load was corresponding to running the described cooling load without expelling any excess heat, resulting in a design heat load of 2230 kW. It is assumed that there is already a storage big enough to mitigate the daily variations in demand.

Table 1: Design conditions for the HPS at 80 % load given by the case study.

Design parameter		Value
Hot water supply temperature	$T_{\text{sink,out}}$	145 °C
Hot water return temperature	$T_{\text{sink,in}}$	110 °C
Cold water supply temperature	$T_{\text{source,out}}$	2 °C
Cold water return temperature	$T_{\text{source,in}}$	8 °C
Design heat load	$\dot{Q}_{\text{heat}}$	2230 kW
Design cooling load	$\dot{Q}_{\text{cool}}$	1380 kW
Lorenz COP	$\text{COP}_{\text{Lor,comb}}$	5.37

2.2. Heat pump modelling

The HPS considered for this case study was an electrically driven vapour compression cycle in a cascade configuration.

The model consisted of an evaporator at the heat source and a desuperheater, condenser and subcooler at the heat sink as visualised in Figure 2 to the left producing hot water at 145 °C and cold water at 2 °C at the sink and source, respectively.

In between the source and the sink, a cascade of two two-stage vapour compression cycles was applied. Both cycles were modelled in a configuration with a bubble-through intercooler minimizing the superheat at the inlet of the high stage compressors. The bottom cycle was modelled with ammonia (R-717) as the refrigerant while the top cycle was modelled with water (R-718) as the refrigerant. The two cycles were connected through a set of cascade heat exchangers (HEX). The first one responsible for desuperheating the ammonia (4→5) while the second HEX was assumed to condense the ammonia (5→6). On the secondary side, the mass flow of R-718 was controlled such that a superheat (ΔT_{SH}) of 0.5 K was ensured at state point 21 shown in Figure 2.

The four compressors (1→2, 3→4, 21→22, and 23→24 in Figure 2) represent a compression process. An isentropic efficiency of 70 % was applied for all compressors, since this value is common for theoretical calculations [8]. The expansion valves (7→8, 10→11, 27→28, and 30→31) were modelled as isenthalpic expansion processes leading the refrigerant into the evaporation process or the liquid separator. The liquid separators (state points 9 and 29) were assumed ideally mixed with pure liquid exiting out the bottom (state points 10 and 30) and vapour leaving with a ΔT_{SH}=0.5 K out the top (state points 3 and 23).

The heat exchangers with ambient air (5a→6a and 11a→11b) were used to expel excess heating or cooling capacity of the HPS. A fraction of the mass flows at point 4 and point 11 went to the ambient air heat exchanger to match demand from the process (see Figure 1). The two ambient air heat exchangers were assumed to always be able to transfer enough heat so the conditions of 6a was equal to 6 and 11b was equal to the conditions of 13.

All heat transfer processes were assumed isobaric. A minimum temperature difference of 5 K was chosen for all the heat exchangers at design conditions as in [9]. The subcooling process in the top cycle (26→27)

and the bottom cycle (6b→7) was maximised so the outlet conditions were set to 5 K above the sink inlet temperature and the ambient, respectively.

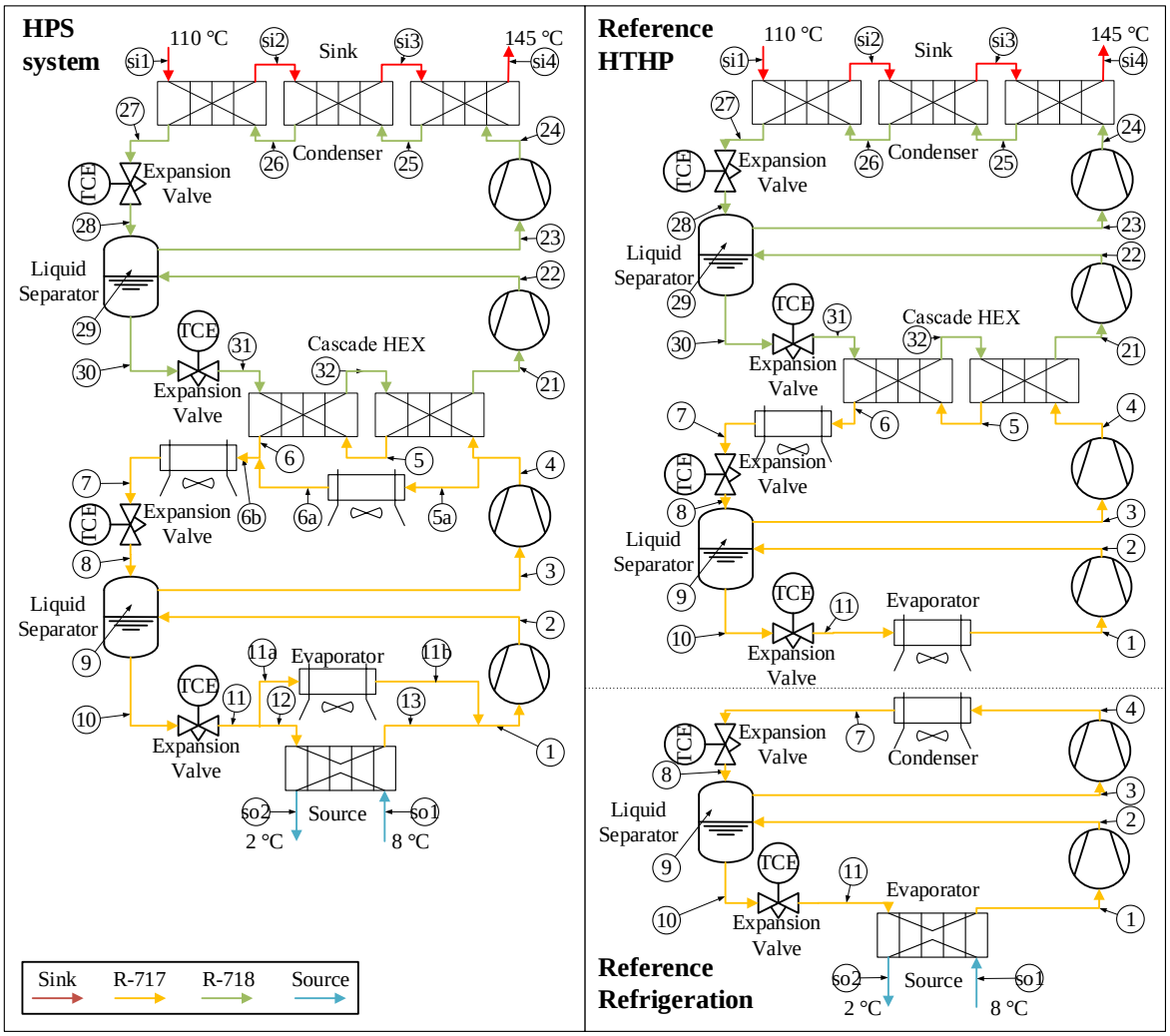

Figure 2:PI-diagram of the combined heating and cooling system, HPS to the left, and the reference systems to the right.

As described, the heat exchangers with ambient air (5a→6a and 11a→11b) were used to expel excess heating or cooling capacity of the HPS to match the process demand. The corresponding control narrative is presented in Table 3 when heat is either in excess or lacking compared to operation according to the design point.

Table 3: Control narrative of the HPS system during different load conditions.

Load conditions	Operational condition
Heat and cooling load is balanced according to design point	The HPS delivers heat to the sink and cooling to the source.
Heat load exceeds excess heat from the cooling system	Absorb heat by operating the air HEX parallel w. the evaporator
Cooling load offering more excess heat then the HP system requires	Expel excess heat by operating the air HEX parallel w. the cascade HEX

A minimum of 0.5 K superheating was considered before the low-pressure compressor of each cycle (point 1 and 21). The condensing temperature of the bottom cycle was optimized for the highest Lorenz efficiency (Equation 2), while fan power pressure losses were neglected. The assumptions at design conditions as in Table 1 are summarised in Table 2.

Table 2: Assumptions for thermodynamic model of the heat pump used in simulations at design conditions as in Table 1.

Component	Assumptions	Value
Evaporator	Pinch point temperature difference	$\Delta T_{\text{pinch}} = 5$ K
	Minimum superheating	$\Delta T_{\text{SH}} = 0.5$ K
Condenser	Pinch point temperature difference in the desuperheater, condenser, and subcooler.	$\Delta T_{\text{pinch}} = 5$ K
	Design heat load	$\dot{Q}_{\text{heat}} = 2230$ kW
Shared cascade heat exchanger	Pinch point temperature difference	$\Delta T_{\text{pinch}} = 5$ K
	Condensing temperature of bottom cycle optimized for highest η_{Lor}	
Heat exchangers with ambient air (5a→6a and 11a→11b)	Same conditions out of HEX as the parallel HEX	$h_{6a} = h_6$ and $h_{11b} = h_{13}$
Air subcooler (6b→7)	Refrigerant maximally subcooled by the ambient temperature.	$\Delta T_{\text{pinch}} = 5$ K
Liquid separator	Intermediate pressures optimized for highest overall η_{Lor}	ΔT_{SH}=0.5 K
	Saturated liquid and slightly superheated vapour towards lower pressure and intermediate pressure side, respectively.	
Compressor	Fixed isentropic efficiency	$\eta_{\text{is}} = 70$ %
Throttling valve	Isenthalpic expansion	
Overall system	Fan power neglected	
	No pressure losses considered	
	R-717 and R-718 used as refrigerants for the bottom and top cycle respectively.	

At the design conditions, the required UA-value of each heat exchanger of the HPS was determined using Equation 1.

$$\dot{Q}_k = (U \cdot A)_k \cdot \text{LMTD}_k \tag{1}$$

Where $\dot{Q}_k$ is the given heat load, $(U \cdot A)_k$ is product of the heat exchanger area and the heat transfer coefficient at design conditions, and LMTD_k is the logarithmic mean temperature difference [10], all for HEX *k*.

During operation at conditions away from the design point, the LMTD changed depending on the heat load experienced by the specific HEX as the UA-values were assumed to be constant.

For the comparison a reference system was modelled as presented to the right in Figure 2. The refence HTHP was modelled using the same configuration as the HPS system with a heat load at design conditions of 2230 kW but utilizing ambient air as an isothermal heat source. Similarly, a refrigeration cycle was modelled for the cold utility. This system was represented by an ammonia cycle like the one shown in the bottom right Figure 2 with the ambient air as an isothermal heat sink. The condensing temperature of the refrigeration cycle was given a lower bound of 10 °C.

The parameter variations are done by varying the total compressor power between 360 kW and 1320 kW and the utilisation of the heat exchangers with ambient air between 0 % and 100 % while optimising the η_{Lor}.

2.3. Performance parameters

For evaluating the performance of the HPS two performance indicators were used. The first one is the power consumption of the compressors while the second was the second law efficiency, η_{Lor}. This was defined as the ratio between the combined COP, COP_{comb}, of the HPS and the maximally achievable COP, as in Equation 2.

$$\eta_{\text{Lor}} = \frac{\text{COP}_{\text{comb}}}{\text{COP}_{\text{Lor,comb}}} \tag{2}$$

Where the $\text{COP}_{\text{Lor,comb}}$ denotes the COP of a Lorenz cycle where both heating and cooling is considered a product at the given boundary conditions defined in Equation 3 [5].

$$\mathrm{COP}_{\mathrm{Lor,comb}} = \frac{T_{\mathrm{sink,av}} + T_{\mathrm{source,av}}}{T_{\mathrm{sink,av}} - T_{\mathrm{source,av}}} \tag{3}$$

With $T_{\mathrm{sink,av}}$ and $T_{\mathrm{source,av}}$ being the thermodynamic average temperatures of the sink and source streams. They are defined as the logarithmic means as in Equation 4.

$$T_{\mathrm{sink,av}} = \frac{T_{\mathrm{sink,out}} - T_{\mathrm{sink,in}}}{\ln\left(\frac{T_{\mathrm{sink,out}}}{T_{\mathrm{sink,in}}}\right)} \qquad T_{\mathrm{source,av}} = \frac{T_{\mathrm{source,in}} - T_{\mathrm{source,out}}}{\ln\left(\frac{T_{\mathrm{source,in}}}{T_{\mathrm{source,out}}}\right)} \tag{4}$$

Here sink out is the hot water supply, sink in is the hot water return, source in is the cold water return temperature, and source out denotes the cold-water supply temperature.

The $\mathrm{COP}_{\mathrm{comb}}$ is defined in Equation 5 as the sum of the supplied heating, $\dot{Q}_{\mathrm{heat}}$, and the supplied cooling, $\dot{Q}_{\mathrm{cool}}$, divided by the sum of each of the compressor's power, $\dot{W}_k$.

$$\mathrm{COP}_{\mathrm{comb}} = \frac{\dot{Q}_{\mathrm{heat}} + \dot{Q}_{\mathrm{cool}}}{\sum \dot{W}_k} \tag{5}$$

The difference in total compressor power of the two solutions, $\dot{W}_{\mathrm{diff}}$, was used as a measure to compare the OPEX of the two solutions. This was defined as the difference in compressor power of the HPS, $\dot{W}_{\mathrm{HPS}}$, and compressor power of the reference system, $\dot{W}_{\mathrm{ref}}$. This is defined as the sum of the compressor power of the high temperature heat pump, $\dot{W}_{\mathrm{HTHP}}$, and reference system refrigeration cycle, $\dot{W}_{\mathrm{refri}}$ as in Equation 6.

$$\dot{W}_{\mathrm{diff}} = \dot{W}_{\mathrm{HPS}} - (\dot{W}_{\mathrm{HTHP}} + \dot{W}_{\mathrm{refri}}) = \dot{W}_{\mathrm{HPS}} - \dot{W}_{\mathrm{ref}} \tag{6}$$

Lastly, the normalized difference in power, $\dot{W}_{\mathrm{diff,norm}}$, is defined using the power of the HPS system at the design conditions, $\dot{W}_{\mathrm{HPS,des}}$ as in Equation 7.

$$\dot{W}_{\mathrm{diff,norm}} = \frac{\dot{W}_{\mathrm{diff}}}{\dot{W}_{\mathrm{HPS,des}}} \tag{7}$$

The performance of the cycles was examined by numerical modelling based on energy and mass balances as described in this section using Python [11] and CoolProp [12] for its thermophysical properties. The minimize function in [13] was used for the optimisation of the COP by changing the condensing temperature of the bottom cycle and the intermediate pressures of both the top- and the bottom cycle. All data was collected, analysed, and visualised using the Pandas library [14].

3. Results

The HPS and the reference system models were used to assess the performance at design conditions for varying ambient temperatures. Additionally, the compressor power at varying heat- and cooling loads were mapped to assess the off-design performance of the HPS compared to the reference system. Finally, the systems were compared in terms of yearly energy consumption using a quasi-steady state approach.

The calculated compressor power of the HPS is presented in Figure 3 as a function of the required heating and cooling load. The utilisation of each heat exchanger with ambient air was varied from 0 % to 100 % in steps of 5 % for all combinations. The total compressor power is varied from 360 kW to 1320 kW in increments of 120 kW. Each grey diamond represents the results of a simulation with a specific utilisation of the heat exchangers with ambient air. The grey curves indicate the pareto fronts in terms of supplied heating and cooling for a specific sum of compressor power. The design point, as defined in Table 1 is marked with a red dot. The simulations were done at an ambient temperature of 20 °C.

The grey curves in Figure 3 are the most efficient operating points for the HPS for a specific combination of demands. The inclination of the grey curves changes with a varying cooling load. At 0 kW cooling load the evaporator is completely bypassed getting all heat for the bottom cycle from the air source. Following the grey curve for 1200 kW compressor power, for higher cooling the potential heat load decreases. This is due to the higher evaporator utilisation increasing the heat load of the component, increasing the LMTD as in

Equation 1. This trend continues until reaching the design point in the steps of about 5 % in correlation with the utilisation of the bottom heat exchanger with the ambient air.

From here, the heat load decreases rapidly for an increased cooling load. This is the second heat exchanger with ambient air bypassing the cascade HEX being used increasingly until the top cycle is fully bypassed. Thereby, the compressor power from the top cycle can be utilised in the bottom cycle instead, hence increasing the potential cooling load. However, the maximal cooling load will reach a maximum, when the bottom cycle compressors reach their maximal operating conditions which are not considered in this study. The remaining combinations of heat exchangers with ambient air utilisation and compressor power yield non-optimal working conditions with lower efficiency.

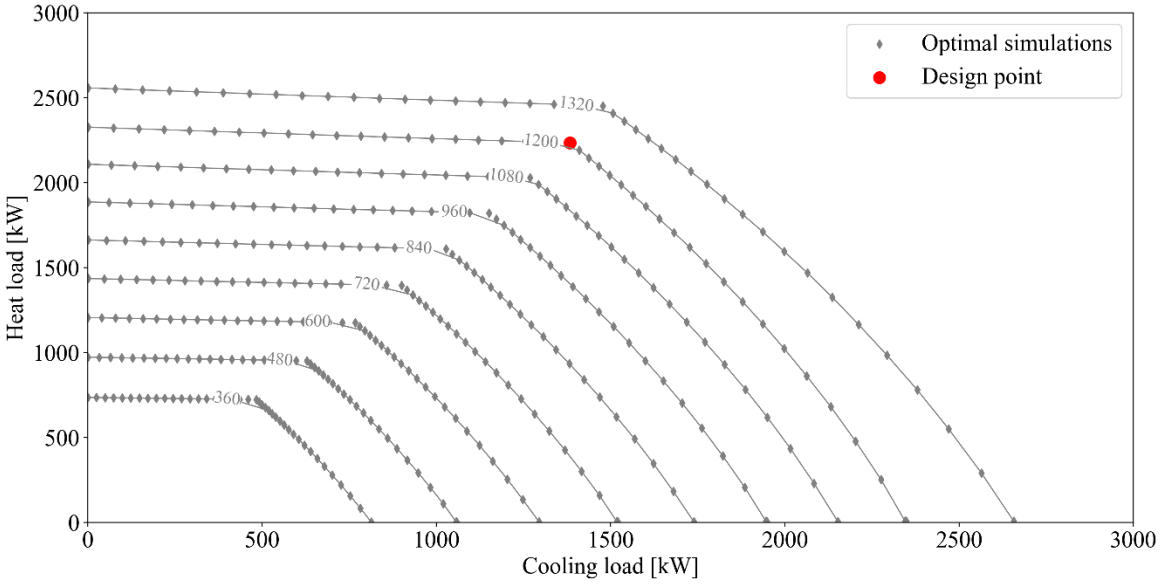

Figure 3: Compressor power at varying heating and cooling loads of the HPS at an ambient temperature of 20 °C.

Similar simulations were performed for the HTHP and the refrigeration cycle as in Figure 3. The normalized difference in compressor power of the HPS and the reference system at the same heating and cooling load is presented in Figure 4. The heat load ranges from 0 kW to 2500 kW and the cooling load from 0 kW to 1750 kW. An ambient temperature of 20 °C was assumed. The result is normalised with the compressor power of the HPS at the design point. Negative $\dot{W}_{\mathrm{diff,norm}}$ indicates a lower compressor power for the HPS. The opposite is true for positive $\dot{W}_{\mathrm{diff,norm}}$, where the HPS will perform worse than the refence HTHP and refrigeration cycle.

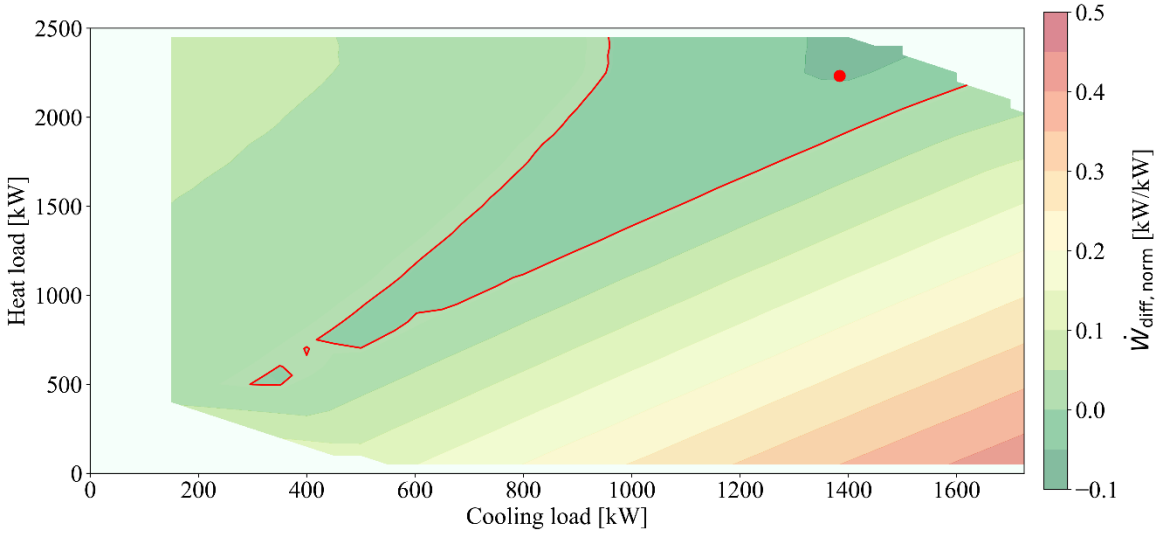

Figure 4: Difference in compressor power of the HPS compared to the separate systems at 20 °C ambient temperature.

From the contour plot in Figure 4 we observe values of $\dot{W}_{\text{diff,norm}}$ between -9.8 % and +47.1 %. The result may be divided into three cases:

- **Heat and cooling load is balanced according to design point:** The efficiency of HPS is higher as shown by the dark green area. $\dot{W}_{\text{diff}}$ is from 0 % to 9.8 % lower for the HPS than for the reference system in this area, with the highest values close to the design point. The area is a wedge shape (outlined with red) spanning from the design point towards the origin. This is as expected since the HPS will operate at similar ratios between the heating and cooling load in this region with minimal usage of the heat exchangers with ambient air.
- **Heat load exceeds excess heat from the cooling system:** The HPS is less efficient than the reference system by up to 10 %. This is due to the expelling of excess cooling which does not significantly affect the power consumption of the HPS as seen in Figure 3.
- **Cooling load offering more excess heat then the HP system requires:** The HPS is less efficient than the reference system by up to 47.1 %. The HPS is penalised comparatively more from an increased cooling load, especially for low heat loads. This is due to the high lift of the bottom cycle compared to the to the reference system.

This indicates, that the HPS will benefit from a high, and stable heat load, where the dark green area is the largest. At the same time, oversizing the HPS will lead to a smaller benefit as the area with negative $\dot{W}_{\text{diff}}$ gets relatively slimmer. A lower cooling load than expected will not hurt the performance as much.

Figure 3-4 show results for constant ambient temperature. This is not the case during yearly operation. Therefore, the effect of varying the air temperatures on the HPS and the reference system was analysed. The performance was evaluated in terms of Lorenz efficiencies at the design point (a heat load of 2230 kW and a cooling load of 1380 kW). The results are shown in Figure 5 both as a function of the ambient temperature and the time of year.

The air temperature affects the two systems differently. The Lorenz efficiency of the HPS (blue) is close to constant for varying air temperatures. This is expected since only the possible subcooling of the bottom cycle is affected by the ambient temperature. η_{Lor} increases for lower temperatures, since a higher subcooling can be obtained. The HTHP and refrigeration cycle (orange) experience a larger effect from the air temperature. η_{Lor} increase with higher temperatures. Higher temperatures result in a larger temperature lift of the refrigeration cycle while the HTHP will overcome a smaller temperature lift. The same is seen through the year (Figure 5 to the right), where the HTHP and refrigeration cycle have a higher η_{Lor} in the summer months, while the efficiency of the HPS is close to constant.

The overall result is the same independent of the ambient temperature. The HPS has a higher η_{Lor} at the design point for every ambient temperature. The difference decreases from 6.24 %p for an ambient temperature of 0 °C to 3.99 %p at 21 °C. This is due to the ambient temperature getting closer to the temperature in the cascade HEX. The HPS has the advantage of being able to optimize the temperature between the two cycles which increases the η_{Lor}. This means that the difference in performance will be more pronounced during the colder months.

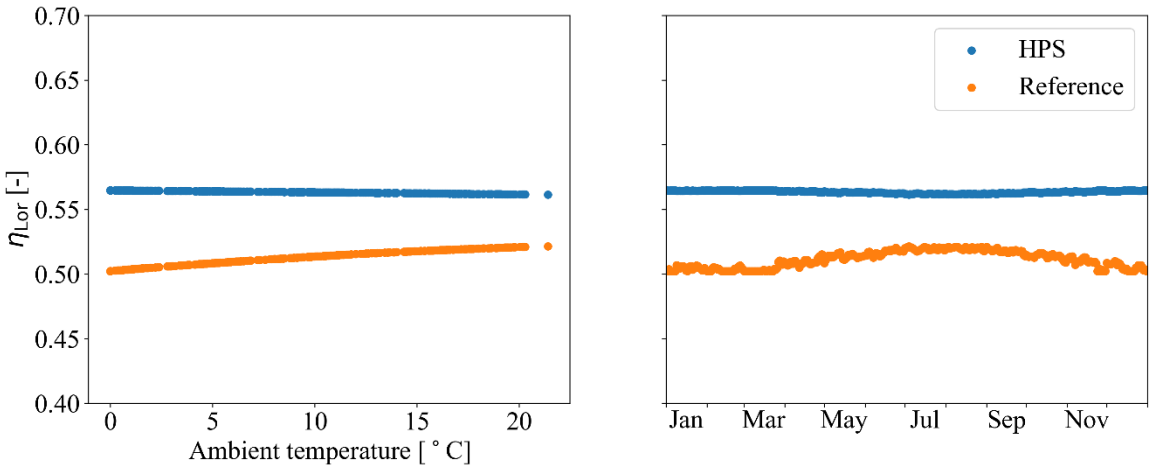

Figure 5: The Lorenz efficiency of the systems at the design loads for varying ambient temperatures (left) and for each of the days of the year of 2021 (right).

In Figure 6 the compressor power of the HPS (blue) is compared to the HTHP and refrigeration cycle (orange) throughout the year 2021. The top figure of Figure 6 shows the compressor power for every day for both solutions. The compressor power varies between 676 kW and 1348 kW for the separate systems and between 684 kW and 1282 kW for the HPS. The biggest differences are during July and August when the HPS has both the highest and the lowest compressor power.

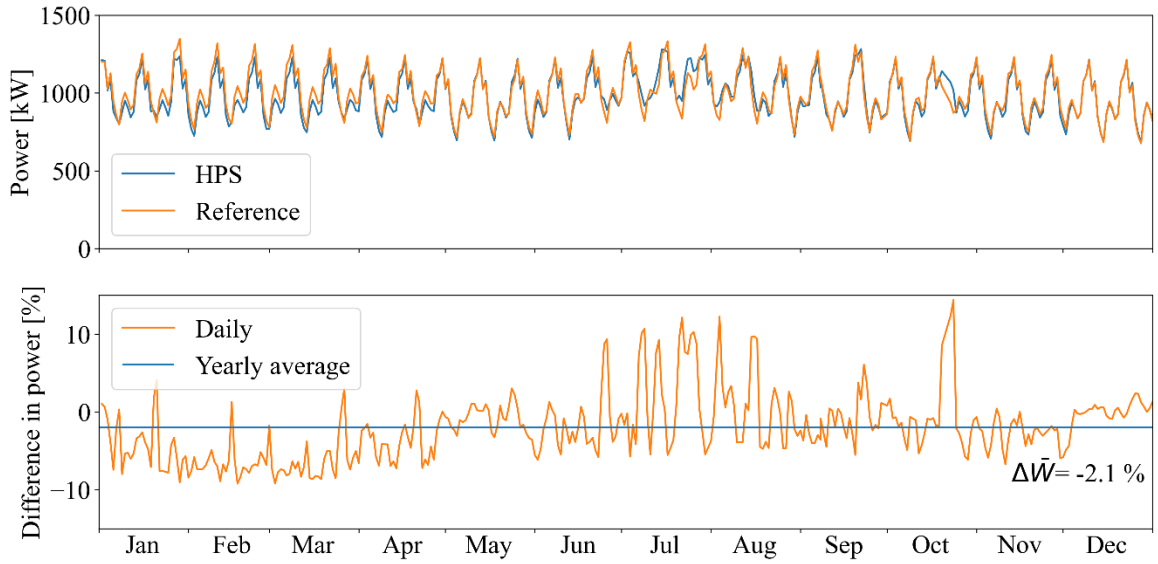

Figure 6: Compressor power of the HPS compared to the HTHP and refrigeration cycle throughout the year 2021. The top figure is the compressor power at every day, while the bottom figure shows the difference in the average power used by the compressors up til that date.

The bottom figure of Figure 6 shows the difference in the compressor power throughout the year. The difference is normalised with the compressor power of the HPS. The blue line indicates the average difference through the year which is 2.1 % in favour of the HPS. The difference in power varies between -9.2 % and 14.2 % being highest in August and the end of October while being lowest in February and March. This is expected as the ratio between the heating and the cooling demand is largest during the winter and smallest during the summer as seen in Figure 1. This yields operating points that are further away from the design point, which is in favour of the separate systems, as shown in Figure 4. Furthermore, the warmer temperatures during the summer months yield a higher η_{Lor} for the separate systems as seen in Figure 5.

4. Discussion

4.1. Alternative configurations of the HPS

The presented HPS is one potential configuration of a vapour compression cycle. Several other refrigerants and configurations could potentially supply the heating and cooling required by the processes. The work in [15]–[17] shows promising performance for heat pumps with hydrocarbons, water, or zeotropic mixtures as the refrigerant with improvements of up to 36 % compared to conventional solutions.

An alternative cycle that could be analysed was presented in [18] utilising two bottom cycles to produce hot and cold water and the top cycle to produce steam. The cycles were connected by a flooded cascade HEX, which additionally acted as a buffer tank. This buffering effect could potentially mitigate some of the penalties of operating away from the design point. The two bottom cycles will, however, introduce further energy demands to consider for a similar study as in this work. Another alternative is the inclusion of a back-up refrigeration cycle with air-cooled condensers or a condenser after the first pressure stage in the bottom of the HPS. This would grant additional cooling capacity with a temperature lift of the ammonia to the ambient temperature instead of the cascade HEX temperature. This will increase the COP following Equation 3 as $T_{\mathrm{sink,av}}$ will decrease.

4.2. Choice of design point

The choice of design point is not trivial and requires full knowledge of the future energy demands. Even when knowing this, it is not possible to choose a design point matching both the heating demand and the cooling demand. By choosing one, the other one is given by the energy balance and the cycle COP. This is in strong contrast to other HPS cycles like in [19] where a CO_2 refrigeration cycle produces space heating as a by-product and cooling as the main product. Thereby, the cooling demand will not define the operating conditions. If the average heating and cooling demand do not correspond to the balanced energy flows of the installed system, off-design conditions will inevitably lead to lower efficiencies for the specific case. In these cases, a HPS will not be suited to deliver the needed heating and cooling without auxiliary equipment. Therefore, more work is needed to determine the optimal design point of the HPS.

4.3. Practical challenges related to the modelled HPS and reference system

The modelled systems were based on a set of decisions that might affect the result. The superheating before all compressors is assumed to be 0.5 K which is normal for flooded evaporators but not for HEX's controlled using thermostatic expansion valves as depicted in in Figure 2. It is not obvious if changing the assumed superheat, will benefit the HPS or the reference system the most. However, the low superheat potentially favours the reference system as it has three evaporators being affected opposed to two for the HPS.

Additionally, the minimum condensing temperature of 10 °C for the ammonia refrigeration cycle potentially implies a two small temperature lift for a 2-stage system. A single-stage cycle could be needed lowering the COP of the cycle, which would favour the HPS. Furthermore, alternative isentropic efficiencies or pinch temperature differences could impact the result.

4.4. Fluctuating heating and cooling demand profiles and potential for the inclusion of storages

As indicated by Figure 4 and 6, the varying demands for heating and cooling substantially lowered the efficiency of the HPS. This was also mentioned by [5], who experienced difficulty delivering the correct amount of heating and cooling simultaneously. The same problem is not addressed by [7], as the HPS only provided 80 % of the heat demand with several backup systems and built-in hot water tanks mitigating the problem, but not leading to full electrification.

An assumption for this study was that all daily fluctuations in the heating and cooling demand profiles could be covered by an already installed storage or buffer capacity. Expanding this assumption with larger storage capacities could mitigate the bi-weekly variations in the heating demand of this case. However, this will require further investigation. Nevertheless, even an infinitely large storage cannot solve this problem if the average heating and cooling demand on a seasonal timescale does fit with the energy balance of the installed system.

4.5. Economic potential

This study showed a 2.1 % decrease in power consumption over a year of operation. This margin indicated that the lower OPEX should not be the only reason for choosing a HPS as the only heating and cooling utility for all industrial cases. It should be noted that fan power has been neglected which will be biggest for the reference system. The operation of large air HEXs could also lead to increased maintenance cost and down-time from required defrosting. Nevertheless, as the HPS had fewer total components than the separate systems, the capital cost could be lower, leading to a better pay-back time on the initial investment. However, the capital cost of the system was shown to be neglectable in [21 - 22] in comparison to the OPEX for high operating hours such as industrial breweries. Therefore, the best solution would allow the HPS to operate at design conditions most of the time while having flexible, auxiliary utilities to cover the variations in demand maximizing the overall efficiency even at higher initial investments.

5. Conclusion

Industrial processes require substantial amounts of energy to cover their heating- and cooling demands. Increased use of electricity in the industry will be necessary for a reduction in the emitted greenhouse gases emitted by the current equipment.

This study evaluated the potential of using a HPS for simultaneously producing hot water at 145 °C and cold water at 2 °C with higher efficiency than a separate HTHP and a refrigeration cycle. The HPS was evaluated by using a case of a Danish brewery with continuous energy demands.

The results showed that the electricity consumption of the HPS decreased by 9.8 % at design conditions compared to a separate heat pump and a refrigeration system. However, the separate systems perform better when the ratio between heating and cooling demand differs substantially from the design point. This trend is more pronounced for low heat loads and high cooling loads. The ambient temperature shows a neglectable effect on the combined system while separate utilities vary by 6 % in Lorenz efficiency.

A yearly quasi-steady simulation showed a 2.1 % lower electricity consumption for the HPS indicating neglectable benefits in terms of operational costs. However, the HPS may present a lower initial investment compared to the supply of heating and cooling individually.

Acknowledgements

This research project was funded by The Energy Technology Development and Demonstration Programme (EUDP), under the project title: “SuPrHeat - Sustainable process heating with high-temperature heat pumps using NatRefs”. The authors are grateful of the financial support from the EUDP and the project partners of SuPrHeat.

Nomenclature

Description (unit)	Symbol	Subscripts and superscripts	Symbol
Heat exchanger area (m^2)	A	Average	av
Coefficient of Performance (-)	COP	Combined heating and cooling	comb
Enthalpy (J/kg·K)	h	Cooling	cool
Logarithmic mean temperature difference (K)	LMTD	Design conditions	des
Efficiency (-)	η	Difference	diff
Heat flow (W)	$\dot{Q}$	Heating	heat
Temperature (K)	T	Into heat exchanger	in
Temperature difference (K)	ΔT	Isentropic	is
Overall heat transfer coefficient ($W/m^2 \cdot K$)	U	Indices	k
Compressor power (W)	$\dot{W}$	Lorenz	Lor
		Normalized	norm
		Out of heat exchanger	out
		Superheating	SH
		Heat sink	sink
		Heat source	source
		Heat pump for simultaneous heating and cooling	HPS
		High temperature heat pump	HTHP
		Pinch point	Pinch
		Reference cycle	ref
		Refrigeration cycle	refri

References

[1] R. de Boer *et al.*, “Strengthening Industrial Heat Pump Innovation: Decarbonizing Industrial Heat,” *Whitepaper*, p. 32, 2020, [Online]. Available: https://www.sintef.no/globalassets/sintef-energi/industrial-heat-pump-whitepaper/2020-07-10-whitepaper-ihp-a4.pdf.

[2] IEA Heat Pump Centre, “Annex 35: Application of Industrial Heat Pumps - Final Report (No. Report HPP-AN35-1&2),” Borås, Sweden, 2014.

[3] R. M. Jakobs and C. Stadtländer, *Final Report Annex 48: Industrial Heat Pumps, Second Phase*, no.

October. 2020.
[4] B. Zühlsdorf, “Annex 58: High-Temperature Heat Pumps,” 2021. https://heatpumpingtechnologies.org/annex58/# (accessed Apr. 18, 2022).
[5] X. D. ZHENG and X. C. LIN, “The Economics of Industrial Heat Pump Systems for Simultaneously Cooling and Heating,” *Heat Pumps*, pp. 327–335, Jan. 1990, doi: 10.1016/B978-0-08-040193-5.50043-2.
[6] P. Byrne and R. Ghoubali, “Exergy analysis of heat pumps for simultaneous heating and cooling,” *Appl. Therm. Eng.*, vol. 149, pp. 414–424, Feb. 2019, doi: 10.1016/j.applthermaleng.2018.12.069.
[7] C. Schlemminger, M. Bantle, and S. Jenssen, “Industrial high temperature heat pump for simultaneous production of ice-water and process-heat,” 2022, doi: 10.18462/iir.gl2022.166.
[8] C. Arpagaus, F. Bless, M. Uhlmann, J. Schiffmann, and S. S. Bertsch, “High temperature heat pumps: Market overview, state of the art, research status, refrigerants, and application potentials,” *Energy*, vol. 152, pp. 985–1010, 2018, doi: 10.1016/j.energy.2018.03.166.
[9] F. Bühler, B. Zühlsdorf, T. Van Nguyen, and B. Elmegaard, “A comparative assessment of electrification strategies for industrial sites: Case of milk powder production,” *Appl. Energy*, vol. 250, no. May, pp. 1383–1401, 2019, doi: 10.1016/j.apenergy.2019.05.071.
[10] F. P. Incropera, *Fundamentals of Heat and Mass Transfer*, 8th ed. John Wiley & Sons, Inc., 2017.
[11] G. Van Rossum and F. L. Drake, “Python 3 Reference Manual.” Scotts Valley, California, 2009.
[12] I. Bell, J. Wronski, S. Quoilin, and V. Lemort, “Pure and Pseudo-pure Fluid Thermophysical Property Evaluation and the Open-Source Thermophysical Property Library CoolProp,” *Ind. Eng. Chem. Res.*, no. 53, pp. 2498–2508, 2014, doi: https://doi.org/10.1021/ie4033999.
[13] P. Virtanen, R. Gommers, and T. E. Oliphant, “SciPy 1.0: fundamental algorithms for scientific computing in Python,” *Nat. Methods*, vol. 17, no. 3, pp. 261–272, Mar. 2020, doi: 10.1038/s41592-019-0686-2.
[14] W. McKinney, “Data structures for statistical computing in python,” in *Proceedings of the 9th Python in Science Conference*, 2010, pp. 51–56, doi: 10.25080/Majora-92bf1922-00a.
[15] M. P. Andersen, B. Zühlsdorf, W. B. Markussen, J. K. Jensen, J. L. Poulsen, and B. Elmegaard, “Thermodynamic analysis of vapour compression heat pump cycles for high-temperature applications,” 2022, doi: 10.18462/iir.gl2022.099.
[16] B. Zühlsdorf, J. K. Jensen, and B. Elmegaard, “Heat pump working fluid selection—economic and thermodynamic comparison of criteria and boundary conditions,” *Int. J. Refrig.*, vol. 98, pp. 500–513, 2019, doi: 10.1016/j.ijrefrig.2018.11.034.
[17] J. K. Jensen, T. Ommen, L. Reinholdt, W. B. Markussen, and B. Elmegaard, “Heat pump COP, part 2: Generalized COP estimation of heat pump processes,” *Refrig. Sci. Technol.*, vol. 2018-June, pp. 1255–1264, 2018, doi: 10.18462/iir.gl.2018.1386.
[18] B. Zühlsdorf, F. Bühler, M. Bantle, and B. Elmegaard, “Analysis of technologies and potentials for heat pump-based process heat supply above 150 °C,” *Energy Convers. Manag. X*, vol. 2, no. January, p. 100011, 2019, doi: 10.1016/j.ecmx.2019.100011.
[19] G. Maouris, E. J. Sarabia Escriva, S. Acha, N. Shah, and C. N. Markides, “CO2 refrigeration system heat recovery and thermal storage modelling for space heating provision in supermarkets: An integrated approach,” *Appl. Energy*, vol. 264, p. 114722, Apr. 2020, doi: 10.1016/j.apenergy.2020.114722.
[20] M. P. Andersen *et al.*, “Economic potential of lowering supply temperatures when using industrial heat pumps,” 2022. In *Proceedings of ECOS 2022 - The 35th International Conference on Efficiency, Cost, Optimization, Simulation and Environmental Impact of Energy Systems 2022*. Copenhagen, Denmark, paper #322.
[21] G. Kosmadakis, C. Arpagaus, P. Neofytou, and S. Bertsch, “Techno-economic analysis of high-temperature heat pumps with low-global warming potential refrigerants for upgrading waste heat up to 150 °C,” *Energy Convers. Manag.*, vol. 226, no. July, p. 113488, 2020, doi: 10.1016/j.enconman.2020.113488.